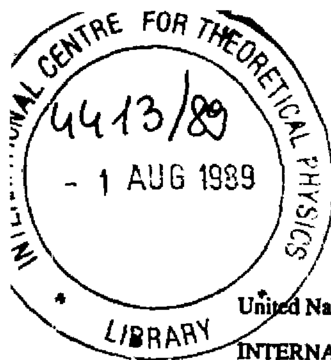
INTERNATIONAL CENTRE FOR THEORETICAL PHYSICS
4413/89
- 1 AUG 1989
LIBRARY
REFERENCE

IC/89/121
INTERNAL REPORT
(Limited Distribution)

International Atomic Energy Agency
and
United Nations Educational Scientific and Cultural Organization
INTERNATIONAL CENTRE FOR THEORETICAL PHYSICS

STRAIN INDUCED AMORPHIZATION OF ALUMINIUM BY MANGANESE IMPLANTATION *

C.A. Majid **
International Centre for Theoretical Physics, Trieste, Italy.

ABSTRACT

The structural modifications of aluminium thin films implanted with manganese ions at room temperature, have been reported. These studies were performed using a two circle X-ray powder diffractometer. The method of X-ray line profile analysis was used to determine strain. As a consequence of ion bombardment, the aluminium lattice was found to undergo distortions. The maximum value of the atomic displacement U_{st} was found to be 0.14 ± 0.01 Å, and the maximum value of the root mean square strain was noted to be $1.05 \pm 0.15 \times 10^{-3}$. The lattice constant a_0 of Al was found to decrease. The decrease in a_0 was noted to be about 0.12 at %.

MIRAMARE – TRIESTE
June 1989

* To be submitted for publication.

** Permanent address: X-Ray Diffraction Group, Nuclear Materials Division, Pakistan Institute of Nuclear Science and Technology (PINSTECH), P.O. Nilore, Rawalpindi, Pakistan.

INTRODUCTION:

In recent years considerable interest has evolved in the production and properties of amorphous metals and alloys both from the fundamental research and applications aspects (Grant and Giesson, 1977; Carter, Colligon and Grant, 1978; Ali et al., 1978; Carter and Grant, 1981; Linker, 1982). Amorphous solids are characterized by the short range order. The long-range periodicity –, a characteristic feature of crystalline solids is absent in these materials. Random or non-crystalline atomic arrangements often result in some unusual physical properties in metallic solids and also support metastable alloy compositions that are not normally found in equilibrium crystalline phase (Grant and Giessen, 1977; Ali et al, 1978; Carter and Grant, 1981). Under these considerations a great effort has been made to develop methods to produce amorphous materials, and to promote an understanding of the amorphization mechanism (Carter and Grant, 1978; Linker, 1982; Carter and Grant, 1982). Different techniques like rapid quenching from the liquid and/or vapour phase or deposition from solutions etc., essentially involve rapid quenching of atomic motion into a stable or metastable static random phase, such that the atoms are not allowed to reorganise into an ordered crystalline state. These methods help to achieve quenching rates in the range from 10^6K to 10^{15}K per second (Grant and Giessen, 1977; Ali et al, 1978; Carter and Grant, 1981).

These techniques have been recently supplemented by the ion implantation method in which energetic ions bombard a crystalline solid. Ion bombardment produces defects due to energy transfer of the penetrating particles to the target atoms in predominantly elastic collisions and displaces target atoms from their positions (Liu et al, 1984, Carter and Grant, 1981). The collision cascades produced by the recoiling target atoms contain highly disordered high temperature zones which collape or 'cool' at extremely high rates, estimated to be around

10^{14}K per second and cause amorphization (Linker, 1981; 1986; Carter and Grant, 1982; Ziemann, 1985). The method of ion implantation offers some unique properties not common to other techniques of amorphization. Only a small amount of material is required. Composition can easily be changed and irradiation parameters are adjustable. The amorphization process can be studied step by step either as a function of fluence in irradiation experiments where particles penetrate a region of interest or a function of concentration when impurities are implanted into a matrix.

Ion induced amorphization has been investigated in detail in various systems (Ali et al., 1987, Linker, 1986; Liu et al.1984; Egami and Waseda, 1984). However, main factors which control the amorphization process remain unclear. Amorphization is a twofold process - growth of amorphous phase and its stabilization. The defect structure and the amount of radiation damage present after bombardment depend on the bombarding conditions like the ion species, its energy and fluence, and on the target material and the substrate temperature. One important parameter concerning preparation of amorphous phase, is the glass forming tendency of a system. Regarding this parameter, different amorphization rules are formulated relying merely on practical experience and theoretically discussed (Carter and Grant, 1982; Liu et al, 1984; Ali et al., 1978). These rules or models are based on the crystalline structure, atomic size and electronegativity etc. of the constituents. These suggestions, nevertheless,at least partially if not completely tend to shed some light on the process. Recently Egami and Waseda (1984) have put forward a model for amorphization of solids. This model is based upon the consideration of local atomic level stresses and focusses on the importance of the atomic size factor in determining the glass forming ability of a system. According to the Egami and Waseda model (1984) strain in a matrix increases upon alloying with increasing the solute concentration. Then if the strain exceeds a critical limit, the matrix would become topologically unstable and might transfer

into the random or amorphous state. The present investigations on the Al - Mn system were undertaken to study if strain plays a role in the amorphization of this system. Further Al - Mn is an important alloy system in that it contains a quasi crystalline phase (Shechtmann etal, 1984). The present investigations are the first of their kind and to the author's knowledge no such information is available in the literature.

Due to limited range of projectiles, ion implantation studies are generally performed on thin layers with thickness of a few thousand Angstroms. In such experiments, to determine structural modifications of films, the grazing angle incidence X-ray diffraction method (Seemann - Bohlin parafocussing conditions or Guinnier thin-film diffractometer) has been considered to be the most suitable (Linker, 1982; 1986). Strain in thin film specimens is then determined using the method of Feder and Berry (1970). In the present investigations, however, we adopted a different approach and present our results on the amorphization of Al thin films under the influence of Mn. Ions implantation, using a two circle X-ray powder diffractometer (the Bragg - Brentano para-focussing geometry). Strain was calculated from the X-ray line profile analysis. In these investigations we show experimentally that strain plays an important role in the amorphization process of a binary system of alloys.

EXPERIMENTAL:

Thin films used in the present investigations were deposited on cleaved single crystal saphire substrates (7 x 25 x 0.5mm) at high vacuum levels ($\sim 2x10^{-9}$ torr). Evaporation rates used were in the range from 200 to 300 Å per second. For the deposition of thin films high purity (99.999 at %) Al was used. These films were not annealed, as perhaps due to the film-surface interaction, any attempt to anneal them resulted into their damage. Mn was introduced homogeneously into the films by multiple energy implanation at room temperature ($\sim$295 K).

Thickness of films and concentration of Mn therein, were determined from the Rutherford backscattering analysis. This was important to estimate the sputtering effects on the film thickness. Fig. 1 shows a typical of such results for a specimen implanted with 4.5 at % Mn. The measured value of Mn concentration in this case was 4.6 at %. The oxygen peak in the spectrum was the contribution from the saphire substrate.

The structural analysis of thin films implanted with Mn ions was carried out using an automatic two circle X-ray powder diffractometer of M/s Siefert , F.R. Germany. The diffractometer was controlled by a computer and used a rotating anode X-ray machine of M/s Siemen,F.R. Germany, for the X-ray source. The machine was operated at 8KW (40 KV x 200 mA) power level. The slit system of the diffractometer was adjusted for the minimum background level and hence the maximum peak to background ratio. The Cu-K_{α_1} radiation (λ = 1.54056 Å) monochromatized by a bent quartz crystal placed in the incident beam was used. Step width used was 0.04^{o} in. The intensity of reflections in the diffraction pattern of Al decreased with Mn impurities. Therefore, to keep the statistical error close to 1 at %, for samples with high concentrations of Mn, long time counting was preferred. Counting time in the range from 10 to 100 second per step was used. To monitor the power output level of the X-ray source, before and after the experiment a standard reference sample (Si-powder) was measured. Also care was taken that only the implanted surface of the sample was exposed to the incident X-rays. This was achieved by using single crystal saphire mask to cover the unimplanted portions of the specimen. The background level on both sides of a reflection was marked over a selected range and then estimated by actually adding the observed counts at each step and average taken. With implantation, hkl reflections in the diffraction pattern tended to become broader. Therefore, to avoid any truncation of peaks, the integration range to calculate integrated

intensities, was carefully chosen. Generally an integration range from 1.75 to 2.5 degree in 2θ was found satisfactory. From these data, the peak centroid and the integral breadth were computed using the procedures described in Bartram (1968) and Klug and Alexander (1974).

STRUCTURAL ANALYSIS:

The as-deposited thin films were always found to contain texture (preferred orientation of crystallites) irrespective of the preparation conditions. Therefore, it was not possible to analyse X-ray intensity in the classical way of comparing the measured to the calculated intensities. A modified procedure was adopted (Linker, 1985; 1986). In this method, the intensities of each single line after implantation was compared to that of the same film before implantation. The intensity of a reflection hkl for a polycrystalline sample before implantation may be expressed as (Linker, 1986).

$$I_o\,(hkl) = K_1 . /F(hkl)/^2\; e^{-2W_1} \qquad (1)$$

with

$I_o(hkl)$ = the intensity of a reflection hkl before implantation.

K_1 = angle dependent constant also containing the amount of material contributing to diffraction.

$F(hkl)$ = structure factor.

W_1 = dynamical Debye - Waller-factor.

After implantation of the specimen, the line intensity may be expressed as:

$$I(hkl) = K_2 . /F(hkl)/^2 . \; e^{-2(W_1+W_2)} \qquad (2)$$

I being the intensity of a particular reflection hkl after implantation. The proportionality constant of equation (1) changes due to material removed by sputtering or partial amorphization. Also here it has been assumed that W_1 does not change by implantation and structural distortions can be described by independent static Debye - Waller factor W_2. Actual atomic displacement values U_{st}

can be obtained from the Debye - Waller factors by using the following relations:

$$W = B \sin^2\theta / \lambda^2 \quad (3)$$

where $$B = 8\pi^2 \langle U_{st}^2 \rangle \quad (4)$$

θ = diffraction angle and λ is the X-ray wavelength.

Taking the ratio of equation (2) and (1) and the logarithm of this ratio leads to the following expression:

$$\ln(\frac{I}{I_o}) = -2B. \sin^2\theta / \lambda^2 + \ln (K_2/K_1) \quad (5)$$

This expression has the form of a straight line if $\ln (\frac{I}{I_o})$ is plotted against $\sin^2\theta / \lambda^2$ and may be referred to as a modified Wilson plot (Linker, 1986). The slopes of such plots give the value B from which average static displacements of the host lattice atoms can be calculated. Here assumption is made that the dynamical behaviour of the lattice is not affected by the distortions introduced in the implantation process. The intercepts of the modified Wilson plots give the ratio K_2/K_1. Since in this ratio, for the same line all angle dependent factors cancel, it contains only the ratio of the material volume contributing to crystalline diffraction after implantation to the material volume contributing to crystalline diffraction before implantation. This volume may change due to partial amorphization and/or material removal by sputtering etc., during implantation. After correction for sputtering effects, therefore, the fraction of the material transformed into the amorphous state can be determined. This analysis procedure is independent of texture effects under the assumption that the texture will not be affected upon ion bombardment (Linker, 1986).

DETERMINATION OF STRAIN:

It is well known that physical parameters such as strain or distortion in the lattice, size of the coherently scattering domains (crystallites) and the experimental diffraction geometry, increase the breadth of reflections in an X-ray powder diffraction pattern (Klug and Alexander, 1974) and X-ray diffraction

lines of sharpness predicted by the diffraction theory, are seldom observed. This feature of the diffraction lines provides a useful means to determine strain and/or particle size of coherently scattering domains from the analysis of the X-ray line profile, provided the profile has been corrected for the instrumental broadening. Strain in a lattice in principle can be determined by either of the following three methods: the Fourier analysis, the method of the variance and the method of breadths of X-ray lines (Bartram, 1968; Klug and Alexander, 1974). In the present analysis, we used the method of breadths of X-ray lines. The present investigations involved analysis of several reflections over the entire range of the diffraction pattern of Al. Also to study the amorphization process step by step as a function of Mn concentrations, analysis of several diffraction patterns was required. Thin films of aluminium (a low scattering metal for X-rays) due to the presence of texture etc., always yielded very weak reflections. Intensities of these reflections decreased continually with each implantation due to reduction of the crystalline aluminium phase. Also because of the amorphization of the sample, these reflections tended to become broad and diffuse progressively with ion implantation. All these factors were likely to render it difficult if not impossible to locate accurately background and/or integration range as demanded by the Fourier analysis and the method of variance. Moreover, the method of variance overemphazes the very unreliable tails of peaks (Klug and Alexander, 1974). The Fourier analysis results because of its involved lengthy computations, has often been used only on the analysis of a single reflection cases (Klug and Alexander, 1974). The sensitivity of the X-ray line breadths method to the choice of integration range and the location of background, on the other hand, is relatively considerably less (Klug and Alexander, 1974). Therefore, in the present investigations, this method was considered to be the best choice. The X-ray lines breadth can be obtained either from the full width at half the maximum (FWHM) of a peak or from its integral breadth which is the area under the peak divided by the peak maximum. The full width at half maximum (FWHM) is undoubtedly a fast and convenient

measurement but unfortunately, it is a very arbitrary quantity and only justified if the profile does not change from one sample to the next. Therefore, in the present studies, the integral breadths of reflections were used in the X-ray profile analysis.

Line broadening resulting from the crystallite effect alone may be expressed by the Scherrer equation (Scherrer, 1918):

$$L = \frac{K\lambda}{B\cos\theta} \qquad (6)$$

where L is the mean dimension of crystallites, B the breadth of the pure diffraction profile; K being a constant, usually set equal to unity λ and θ are the X-ray wavelength and the diffraction angle, respectively. Equation (6) may be written as:

$$\Delta s_p = \frac{K}{L} \qquad (7)$$

with $\Delta s_p = \frac{(2\cos\theta)\cdot\Delta\theta}{\lambda}$; and $s = \frac{2\sin\theta}{\lambda}$

Here B has been set equal to $\Delta 2\theta$.

According to Wilson (1949), the integral line breadth generated by distortions or strains alone can be expressed by the following equation:

$$\Delta s_D = \frac{4e\sin\theta}{\lambda} = 2es \qquad (8)$$

where e is the maximum strain parameter. The subscripts p and D are indicatives of the size effect and the distortion effect, respectively.

Theoretical considerations and experimental results both tend to show that strain broadening may usually be approximated rather well by a Gaussian function, whereas the effects of small crystallite size more closely resemble a Cauchy broadening profile. The experimentally observed profiles are actually never pure Gaussian or pure Cauchy (Klug and Alexander, 1974), suggesting perhaps the presence of both strain and size effect. The integral breadth of the convolution of a Gaussian function of breadth B_G and a. Cauchy function of breadth B_c

according to Halder and Wagner (1966) may be expressed by the parabolic relationship:

$$\frac{B_c}{B_o} = 1 - \left(\frac{B_G}{B_o}\right)^2 \qquad (9)$$

B_o' being the observed integral breadth of a line.

For Cauchy size broadening and Gaussian strain broadening, then

$$B_s/B_o = 1 - \left(\frac{B_D}{B}\right)^2 \qquad (10)$$

Substitution of equations (7) and (8) in equation (10) gives

$$\frac{K}{\Delta s_o L} = 1 - \frac{4e^2 s^2}{\Delta s_o^2} \qquad (11)$$

which can be easily converted to the following from in terms of the integral breadth $\Delta 2\theta$ (radians) of a reflection hkl (Klug and Alexander 1974):

$$\frac{(\Delta 2\theta)^2}{\tan^2\theta_o} = \frac{K\lambda}{L}\left(\frac{\Delta 2\theta}{\tan\theta_o \cdot \sin\theta_o}\right) + 16e^2 \qquad (12)$$

Here θ_o is the maximum peak position, e the maximum strain.

From equation (12), the particle size and the strain can be computed by using any available multiple orders of a given reflection hkl to construct linear plots of $\frac{(\Delta 2\theta)^2}{\tan^2\theta_o}$ vs $\frac{\Delta 2\theta}{\tan\theta_o \sin\theta_o}$ as a function of impurity concentration. The slope of such plots yield the quantity $K\lambda/L$ from which L can be calculated. The intercepts of these plots on the ordinate give the quantity $16e^2$. The maximum strain thus obtained may be replaced by the lattice distortion parameter like the root mean square strain $\langle \varepsilon^2 \rangle^{1/2} = \frac{e}{1.25}$ (Klug and Alexander, 1974). The integral breadth $\Delta 2\theta$ in equation (12) free from instrumental broadening was obtained from the experimentally observed breadth B by unfolding from the instrumental broadening b, using the parabolic correction method of Warren (1949). This is expressed by the following equation:

$$\frac{\Delta 2\theta}{B} = 1 - \left(\frac{b^2}{B^2}\right)^{1/2} \qquad (13)$$

The instrumental breadth can in principle be obtained experimentally using a standard sample with minimum strain and having particle size in the range from 1-10 μ. The absorption coefficient of the standard sample used must be close to that of the experimental one (Bartram, 1980; Klug and Alexander, 1974). It is however, the best to use a standard sample of the same material as the one under investigation (Klug and Alexander, 1974). In the present studies therefore, a thin film of aluminium which gave the minimum values of integral breadths for various reflections in the powder diffraction pattern, after the first implantation at 0.5 at % of Mn, was used as a standard to correct for the instrumental broadening. Such samples were found to have the minimum strain. Fig.2 shows a plot of integral widths of a typical such sample.

RESULTS AND DISCUSSION

Results of these investigations are illustrated in Figures 3 to 10. The aluminium thin films used in these studies had a polycrystalline FCC structure. The unit lattice parameter a_o was found to be 4.0490 ± 0.002 Å-, a value close to that for the bulk material (a_o = 4.0494 Å, (Swanson and Tatge, 1953). The grain size of these films before Mn implantation was determined to be about 900 Å. Typical X-ray diffraction spectra of these films before and after their implantation, up to $2\theta = 84^o$ are shown in Fig. 3. The X-ray diffraction spectrum (a) in this figure was recorded before the Mn implantation. This spectrum clearly shows well resolved hkl reflections for the FCC structure of Al. As is obvious from other spectra (c to d), the implantation of Mn ions did not change this FCC structure; but the intensity of reflections decreased substantially at each implantation and peaks tended to become broader until their intensity became so small that they disappeared into the background. It was the high angle reflections which disappeared from the spectrum first. Fig. 3 also shows a very broad band around $2\theta = 60^o$. As is obvious from the other spectra, this band tends to grow with implantation of Mn ions. This was contributed by the saphire substrate perhapes due to its damaged surface under the influence of ion bombardment. As a consequence of Mn implantation, growth of an amorphous phase was observed to proceed gradually. At about 8 at % of Mn concentrations, when the specimen under investigation was amorphized to the extent of about 60 at %, close to the position of Al (111) reflection (Fig.3 a) a broad band, characteristic of amorphous phase, with the (111) reflection superimposed upon it, made its appearance. With further implantations, this band increased and the intensity of (111) reflection decreased until around 20 at % of Mn concentration, when the specimen under investigation was amorphized almost completely.

Modified Wilson plots for various concentrations of Mn are shown in Fig.4. Straight lines have been fitted through the points though some scatter appears in the data. These curves have two main features, namely, slopes of the lines and their intercepts on the ordinate. As mentioned earlier, the slopes of these lines indicate distortions of the crystalline structure, which if described by small static displacements of the atoms yield the root mean square amplitude of these displacements. As is obvious from Fig.4, little or no change in the slopes of the modified Wilson plots was observed up to about 2 at % of Mn concentration, suggesting the absence of atomic displacements. However at 2.5 at % of Mn concentrations, these curves showed a gradual increase in their slopes up to about 0.65 at % of Mn concentrations. With further implantation of Mn ions, slopes of the modified Wilson plots simply leveled off or even tended to decrease. These features suggested that implantation of Mn ions into Al at room temperature, do not bring about any appreciable change in the atomic displacements U_{st} of the atoms of the host lattice up to about 2 at % of Mn impurity. However, as Mn concentrations are increased further the host lattice is perturbed more and more strongly and the atomic displacement U_{st} tends to increase with increasing Mn concentrations, attaining a maximum value arround 6.5 at % of Mn concentrations. Any

increase in the Mn concentrations, above this limit does not seem to have any effect on the parameter U_{st}. This is shown in Fig. 5, which illustrates the plot of U_{st} vs. C, the Mn concentrations. The maximum value of the atomic displacements U_{st} observed in the present investigations, was 0.140 ± 0.010 Å.

In Fig. 6, the percentage growth of the amorphous phase, computed from the intercepts of the modified Wilson plots (Fig.4) is plotted against Mn concentration C. As is obvious from the plot, there was little or no evidence for the growth of an amorphous phase below 2 at % of Mn impurity. However, around 2.5 at % of Mn concentrations, amorphization of the specimen became evident and increased almost linearly up to about 12 at % of Mn concentrations. At this concentration level approximately, 75 at % of the specimen was vitrified. Further implantation resulted into a rather slow growth of the amorphous phase. This is evident from Fig.6. The percentage of amorphization vs Mn concentration C curve tends to show saturation. Complete amorphization of the sample was achieved around 20 at % of Mn concentration C -, relatively over a wide range of composition. The saturation region was thought to be artificial concerning the Mn concentration for total amorphization in that respect here most of the implanted Mn is deposited into regions which are already amorphous and only a small fraction is passed into still crystalline material where critical threshold values (discussed in the following) of the Mn concentrations, have not been yet reached. The average composition of the new amorphous phase/compound was estimated to be about Al_{87} Mn_{13}, astonishingly close to the composition which is reported to grow into a quasi crystalline phase (Shechtaman et al., 1984). The wide range of composition over which amorphization of the specimen was observed at room temperature, could perhaps be reduced if implantation was made at liquid nitrogen temperature due to the following reason. Amorphization is a two fold process, viz., growth and stabilization (Carter and Grant, 1981; 1982). At room temperature, the destabilizing forces are large and all the amorphous phase grown may not stabilize whereas at liquid nitrogen temperature, this is less likely

to happen. The defect (vacancy) mobility which influences the transition into the amorphous state, is expected to be greater at room temperature (Grant and Giessen, 1977; Carter and Grant, 1981; 1982). The greater defect mobility is expected to assist in the destabilization of the grown amorphous phase.

The lattice constant a_o of the host lattice was found to change under the influence of the ion bombardment. Initially up to about 6 at % of the Mn concentration C, a_o was found to decrease though not very strongly and then suddenly increase (to almost the same value, as that for the bulk material) as the implantation of Mn ions was proceeded.
This is shown in Fig. 7 which illustrates the plot of a_o vs. C. The change, however, was small and the maximum deviation noted was about 0.12 at %. It may be interesting to note that the value of Mn concentrations at which the lowest lattice constant a_o was obtained, correspond closely to the critical value of concentrations of Mn ions at which maximum value of the atomic displacements parameter U_{st} was observed. Also this was the concentration level of Mn impurities around which the maximum value of the root mean square strain $\langle \varepsilon^2 \rangle^{1/2}$ (the lattice distortion parameter), was found. Implantation of Mn ions into the host lattice, above 6.5 at % of Mn concentrations, resulted into the release of strains. This is discussed in the following. The observed decrease in the lattice constant a_o and hence the contraction of the host Al lattice under the influence of the Mn implantation my be understood in terms of Mn atoms (atomic radius = 1.30 Å; Pauling, 1962) probably going to the substitutional sites by knocking out the Al atoms (atomic radius = 1.43 Å; Pauling, 1962). To accomodate Mn atoms which tend to replace Al atoms, relatively less space would be required and hence the host lattice may tend to contract. Nevertheless, to confirm this hypothesis more experiments to determine the substitution coefficient of Mn atoms into the Al lattice are required to be performed.

Fig. 8 illustrates the plots of $\frac{(\Delta 2\theta)^2}{\tan^2\theta_0}$ vs $\frac{\Delta 2\theta}{\tan\theta_0 \cdot \sin\theta_0}$ for different concentrations of Mn. A careful examination of these curves reveals their two main features, viz., the slope and their interceptions on the ordinate. From the slopes of these curves we obtained the particle size L of the coherently scattering domains as a function of impurity concentration C, through the quantity $\frac{K\lambda}{L}$ simply by setting the constant K equal to unity (Klug and Alexander, 1974), being the wavelength of the Cu $K\alpha_1$ radiation used. The first implantation of the as-deposited Al film caused the slope of such a curve at 0.5 at % of Mn concentration to decrease. The particle size was therefore found to increase from about 900 Å for the as - deposited film to about 1000 Å with the implantation. However, with subsequent implantations slope of these curves increased into a continous fashion suggesting a continuous decrease of the grain size. This is shown in Fig. 9 which illustrates the variation of the grain size with Mn concentrations. The minimum particle size thus obtained was around 250 Å. This was observed at about 12 at % of Mn concentrations. No further appreciable change in the particle size was observed. It tended to saturate around this value. The accuracy of measurements was about 15 at %.

The intercepts of various curves shown in Fig. 8 initially increased with implantation of Mn impurities upto about 6.5 at %. By further implantation, the interceptions tended to decrease sharply to almost zero around 8 at % of Mn concentration. The interceptions of these curves on the ordinate are a measure of the strain. Therefore this feature of curves in Fig. 8 suggests that Mn concentrations initially increase the strain up to some critical values - that by further implantation, strains are released. Fig. 8 also reveals another interesting feature regarding behaviour of Al films toward strains. Here in this figure, besides two orders of the (111) reflection other hkl reflections in the diffraction pattern of the Al thin film are also plotted. As is obvious from Fig. 8, points due to all these

reflections also fall nicely on the same line as drawn through the points for the reflection (111) and the reflection (222), with of course some spread of the data, which may be due to the error in the determination, of integral widths. This feature indicates that the Al films were isotropic as regards the distribution of strain.

The root mean square strain $\langle \varepsilon^2 \rangle^{1/2}$ computed from the interceptions of plots at various concentration of Mn in Fig. 8, is plotted in Fig. 10 as a function of implanted Mn concentration C. These data show a linear increase of strain with Mn concentration C up to about 6.5 at %. By further Mn implantation the measured root mean square strain values decreased to almost zero at about 8 at % of Mn concentration. The maximum value of the strain computed from these investigations was $1.05 \pm 0.15 \times 10^{-3}$.

The results of the present investigations may be interpreted as follows. Due perhaps to relatively poor solubility of Mn into Al at room temperature, as a consequence of ion implantation, a supersaturated solid solution may be expected to be formed. Under the ion bombardment, the forced introduction of Mn then causes distortion of the host lattice which could be described by small static displacements of the lattice atoms as well as accumulation of strain. At a critical strain value which corresponds to a critical Mn concentration the matrix undergoes a phase transformation into the amorphous state. This transition develops over a certain concentration range since due to the statistical fluctuations in the distribution of the implanted impurities, their will be regions in the film reaching the critical values earlier or later (Linker, 1986). This conclusion is supported by the fact that the lattice parameter a_o remains constant in the crystalline rest - material upon amorphization. The release of strain by implantation beyond 6.5 at % Mn concentrations, may be explained as follows. After exceeding the critical value for amorphization, and upon amorphization, strains are determined in the crystalline rest - material with a subcritical Mn concentration and therefore lower strain values.

The fact that the total volume of the specimen was not transformed into the amorphous state emphasizes the twofold role of impurities in the amorphization process, viz; initially the build-up of strains on the lattice sites and then upon transformation, the stabilization of the amorphous phase. At a concentration of 6.5 at % for the Al-Mn system under present studies, only those regions transform which, presumably also locally contain a critical impurity concentration for stabilization. Also the partial amorphization observed at low impurity concentrations in the present case, may be caused by the high quenching rates from dense cascades (spikes) which are equally likely because of the heavier Mn projectiles (Linker, 1986; Ziemann, 1985; Carter and Grant, 1982). The observation of a continuous accumulation of strain and spontaneous transition into the amorphous state is in principle, in accordance with the defect accumulation model. Coterill (1977) has shown that the dislocation density in a metal is limited and that a rearrangement of the atoms occurs when the dislocation density exceeds a threshold value. The increase of the defect density in a metal can be associated with strain accumulation. This strain accumulation according to Egami and Waseda (1984) is only a necessary condition for amorphization. It will depend on the system under investigation and the experimental conditions whether it is really achieved. Implantation of Mn into Al at room temperature suggests that defect mobility influences the transition into the amorphous state, it is likely to occur at higher concentration compared to the liquid nitrogen temperature.

CONCLUSIONS:

Analysis of structural modifications and/or the amorphization process in Al thin films under the influence of Mn ions implanted at room temperature, has been carried out using a two circle x-ray powder diffractometer (Bragg - Brentano parafocussing geometry). Measurement of strain and grain size as function of Mn concentrations was accomplished using the method of x-ray line profile analysis.

The forced introduction of Mn ions into the Al lattice, causes the lattice constant to decrease. Strain and static atomic displacements increase with implantation up to a certain critical level. By further implantation, strains are released and the atomic displacements tend to saturate. Also the lattice constant regains its pre-irradiation value as soon as the strains are released. Grain size decreases with increasing Mn concentrations in a continuous fashion. Complete amorphization of the sample was observed around 20 at % of Mn impurities. The greater defect mobility at the room temperature conditions, seems to influence the phase transformation transition from the crystalline to the amorphous state - it occuring over relatively a wider range of composition. These investigations clearly underline the usefulness of a two circle x-ray powder diffractometer for such investigations.

ACKNOWLEDGMENTS

The author would like to thank Professor Abdus Salam, the International Atomic Energy Agency and UNESCO for hospitality at the International Centre for Theoretical Physics, Trieste.

REFERENCES:

1. Ali, A., Grant, W.A. and Grundy, P.J. (1978) Phil. Mag. B-37 No.3, pp. 353 - 376.
2. Bartram, S.F. (1967) in: Handbook of X-Rays (McGraw - Hill, N.Y., Edit.: E.F. Kaelble) p: 17-1 - 17.18.
3. Carter, G. and Grant, W.A. in: Proc. Int. Conf. Amorphous Systems Investigated by Nuclear Methods (Edits. Kajcsos, Zs; Dezsi, I, Harvath, D., Kemeny, T., Marczis, L and Nagy D.L., Balatonfüred , Hungrey, 31 August - 4 September, 1981) p. 49.
4. Carter, G. and Grant, W.A. (1982) Nucl. Inst. Methods, 199, pp. 17-35.
5. Coterill, R.M.J. (1977) Phys. Lett. 60A, p. 61.
6. Egami, T and Waseda Y. (1984) J. Non-Cryst. Solids 64, pp. 113-134.
7. Feder, R. and Berry, B.S. (1970) J. Appl. Cryst. 3, pp.372-382.
8. Grant, N.J. and Giessen, B.C. (1977) Rapidly Quenched Metals (M.I.T. Press, U.S.A.).
9. Halder, N.C. and Wagner, C.N.J. (1986) Acta Cryst. 20, p 312.
10. Holz, M., Ziemann, P. and Buckel, W. (1983) Phys. Rev. Lett. 51 No.17, pp. 1584-1587.
11. Klug, H.P. and Alexander, L.E. X-ray Diffraction Procedure for Polycrystalline and Amorphous materials (John-Wily, N.Y.) (1974).
12. Linker, G. (1986) Vacuum, 36 Nos. 7-9, pp. 493 - 501.
13. Linker, G.(1982) in: Ion Implantation Into Metals (Edit. Aschworth, V, Grant, W.A, Procter, R.D.M., Pergamon Press, Oxford) P.284.
14. Linker, G.(1986) Solid. State Commun. 57 No.9, pp. 773 - 776.
15. Linker, G.(1985) Mat. Sci. & Eng. 69, pp. 105 - 110.
16. Liu Bai-Xin, Johnson, W.L. and Nicolet, M.A. (1983) Nucl. Inst. & Methods, 209 - 210, pp. 229 - 234.
17. Pauling, L.(1962) The Nature of Chemical Bond (Verlag Chemie GmbH, Weinheim/Bergstr., FRG).
18. Scherrer, P. (1918). 2, p. 98.
19. **Swanson and Tatgo (1950) Joint Committee on Powder Diffraction Standards (JCPDS) Card No.0787 File No.4.**
20. Shechtman, D., Blech, I., Gratias, D. and J.W. Cahn (1984) Phys. Rev. Lett. 53, p 1951.
21. Wilson, A.J.C. (1949) X-Ray Optics (Methuen, London) pp. 37-40.
22. Warren, B.E. (1941) J. Appl. Phys. 12, p. 375.
23. Ziemann, P. (1985) Mat. Sci. & Eng. 69, pp. 95 - 103.

FIGURES CAPTIONS

Fig. 1 . Rutherford backscattering curve for the analysis of a typical thin film containing 4.5 at % of Mn.

Fig. 2 . Variation of the integral peak width of the X-ray line profile as a function of the diffraction angle 2θ .

Fig. 3 . X-ray diffraction pattern of the film implanted with different Mn concentrations.

Fig. 4 . Modified Wilson plots for an aluminium thin film implanted with different Mn concentrations.

Fig. 5 . Variation of atomic displacements U_{st} as a function of Mn concentrations in aluminium.

Fig. 6 . Percentage growth of amorphized aluminium as a function of Mn concentrations.

Fig. 7 . Variation of the lattice constant a_0 as a function of Mn concentrations.

Fig. 8 . Plots of $\left(\frac{\Delta 2\theta^2}{\tan^2\theta}\right)$ vs. $\frac{\Delta 2\theta}{\tan\theta_0 \cdot \sin\theta_0}$.

Fig. 9. Variation of the particle size in an aluminium film as a function of Mn concentrations.

Fig. 10 . A plot of the root mean square strain $\sqrt{\overline{\varepsilon^2}}$ vs. Mn concentrations in aluminium thin film.

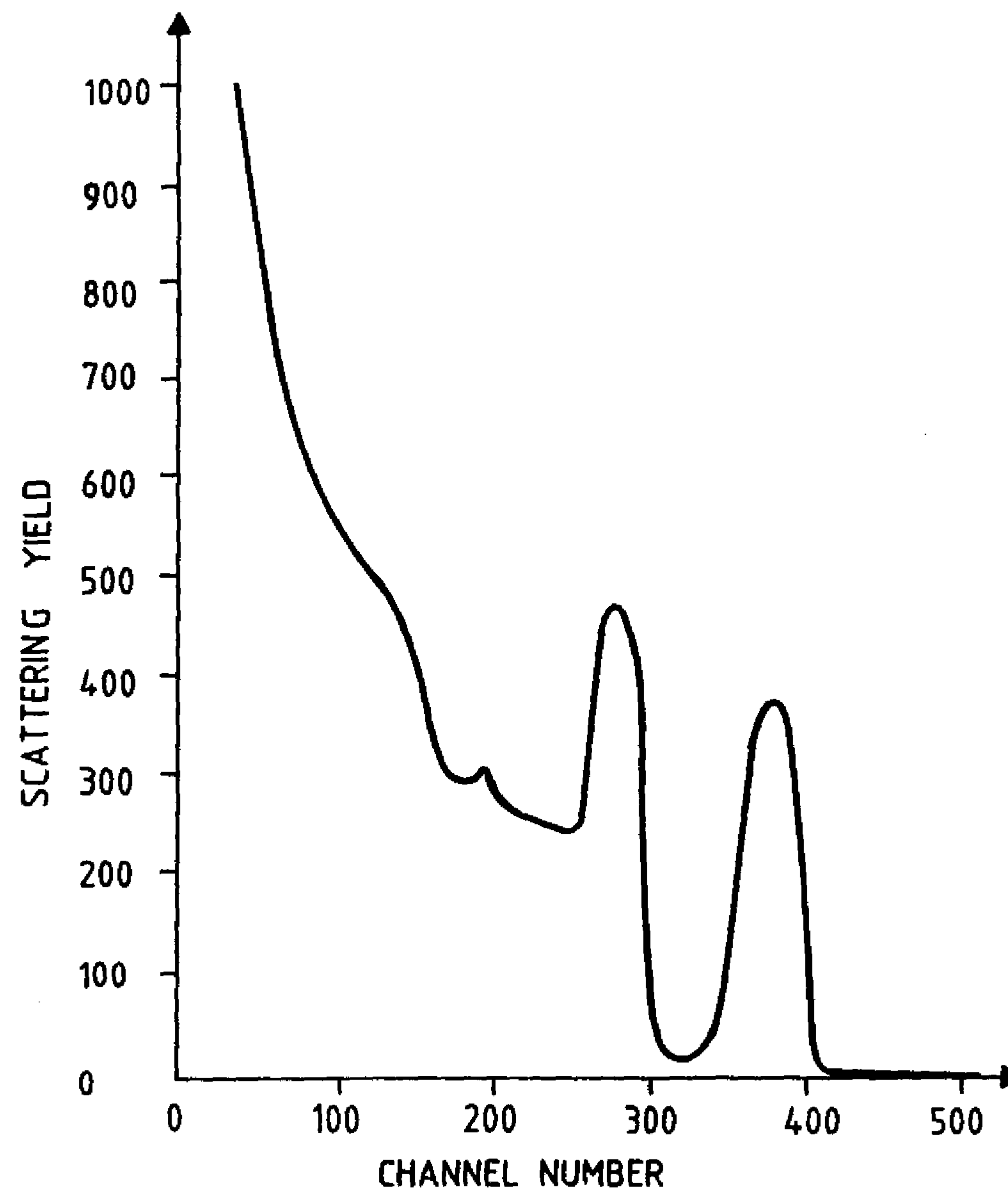

Fig. 1

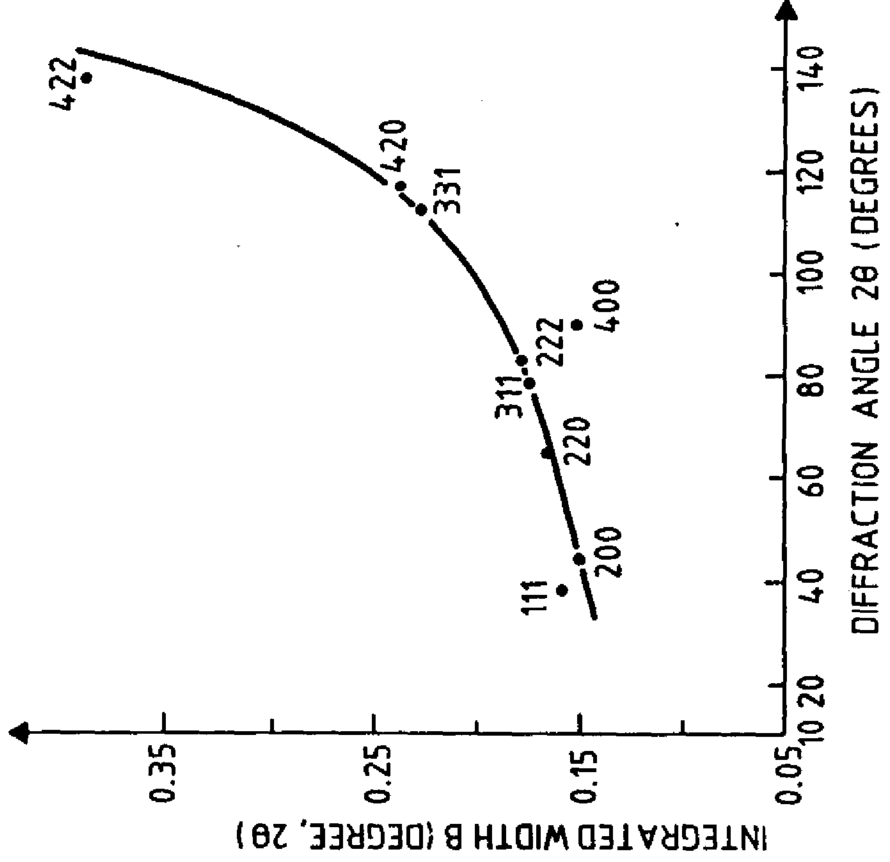

Fig. 2

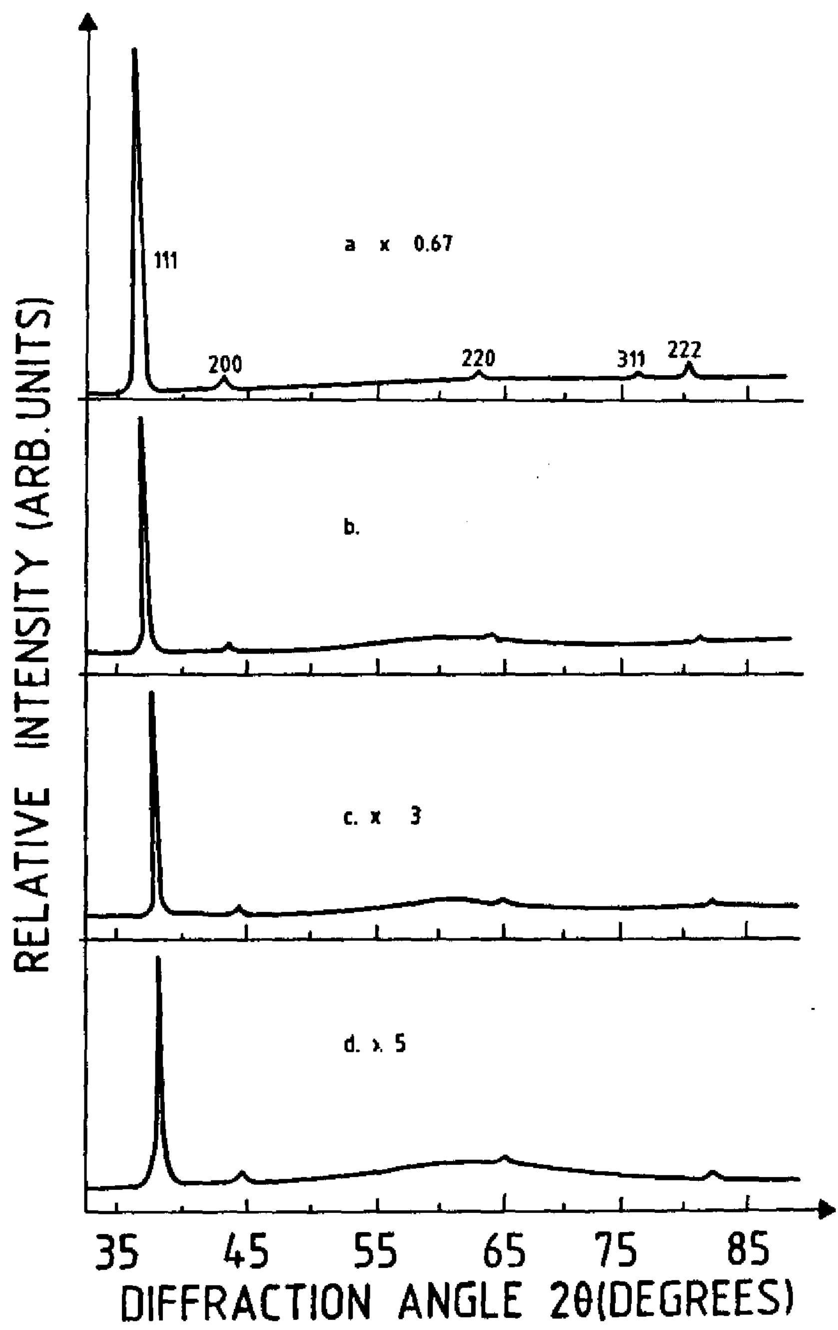

Fig. 3

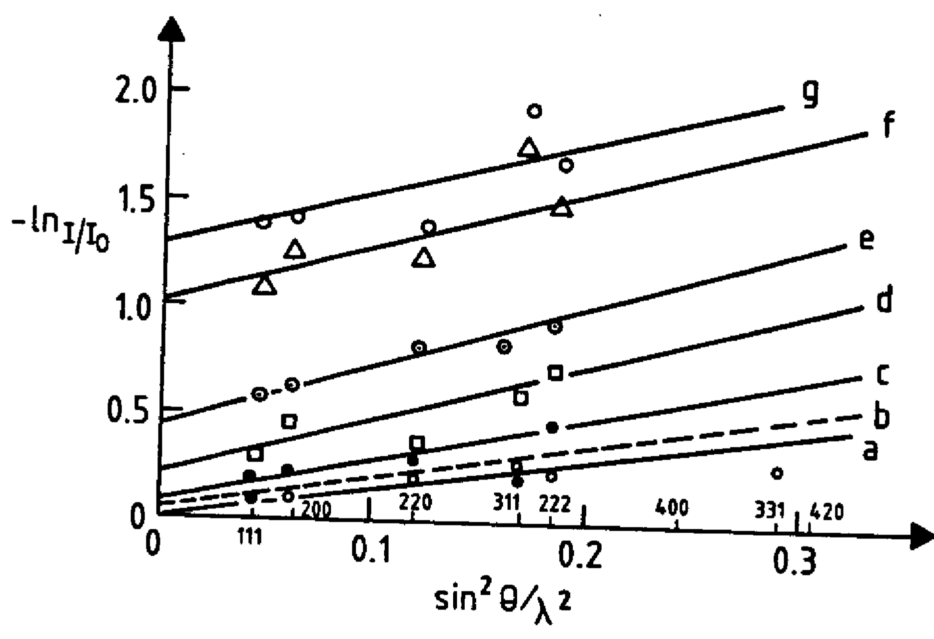

Fig. 4

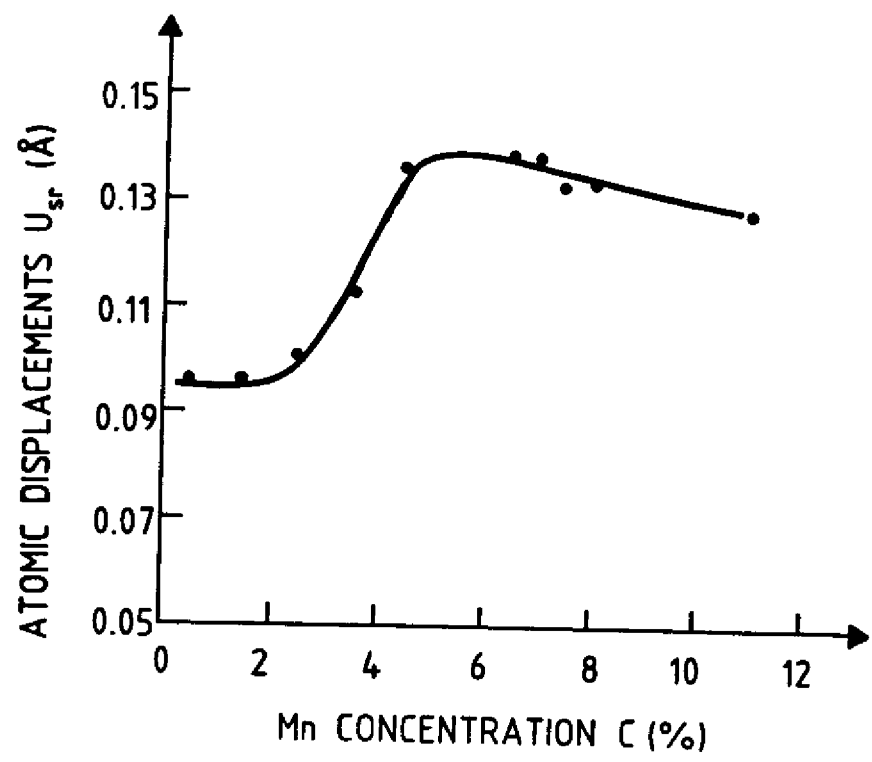

Fig. 5

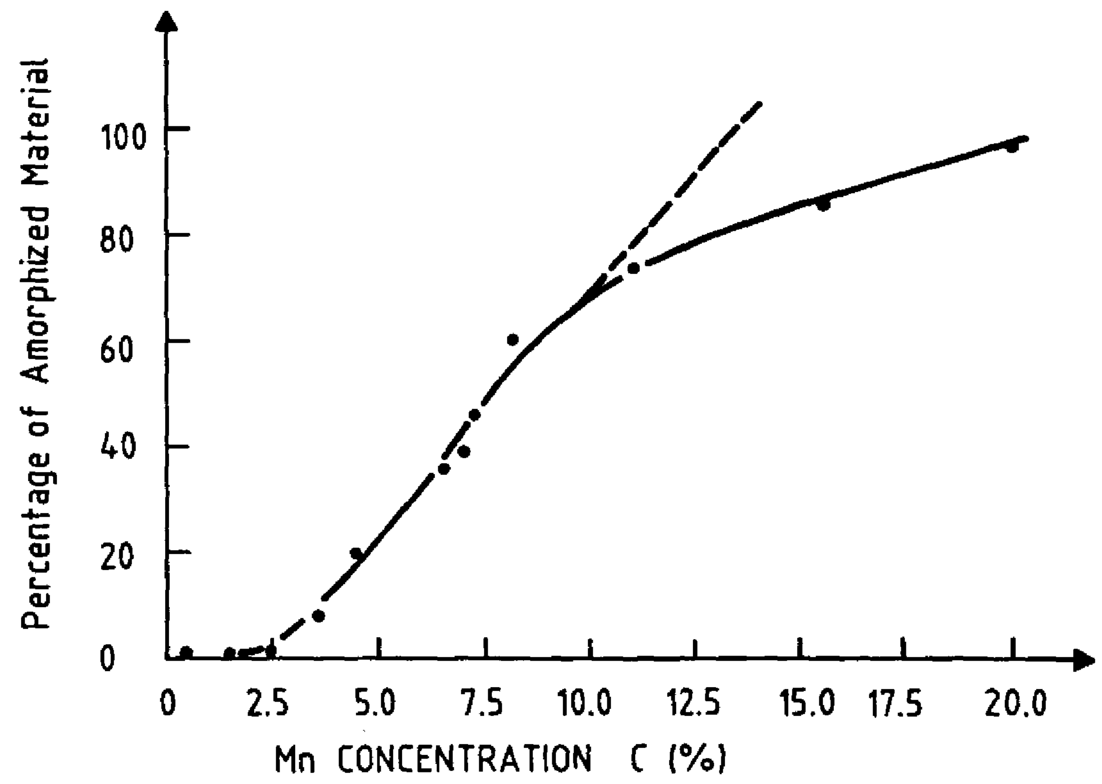

Fig. 6

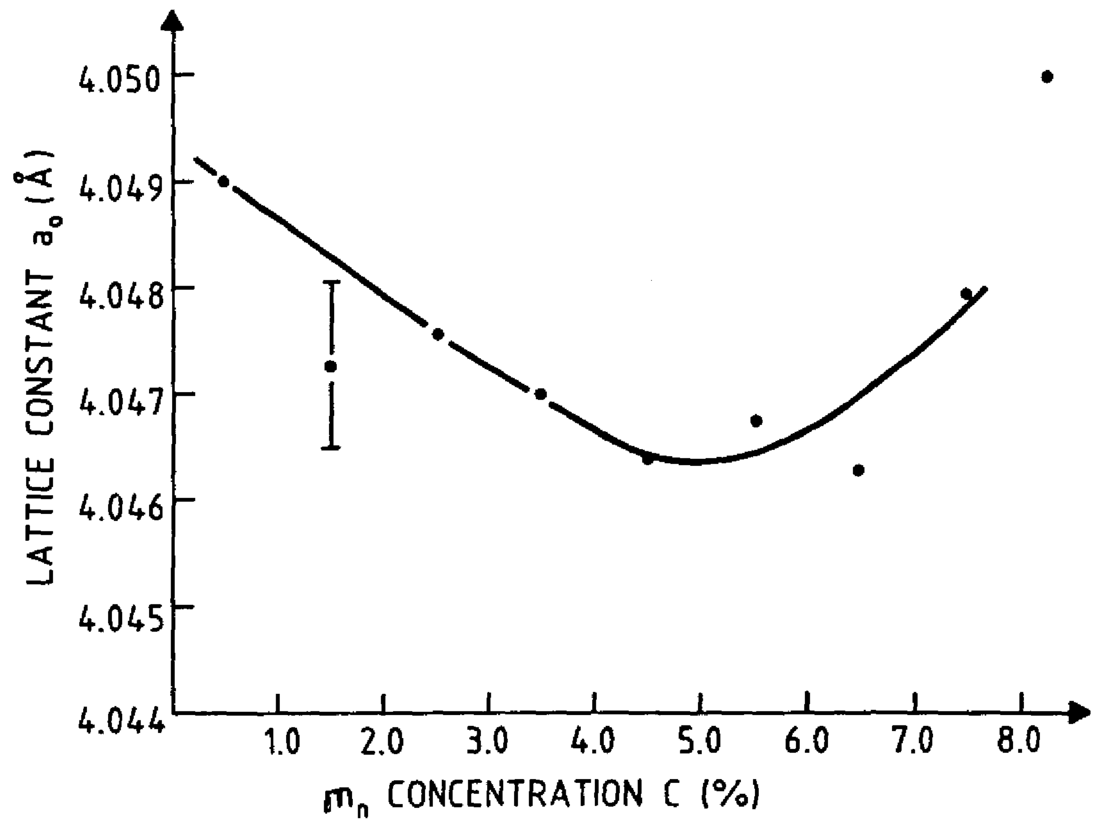

Fig. 7

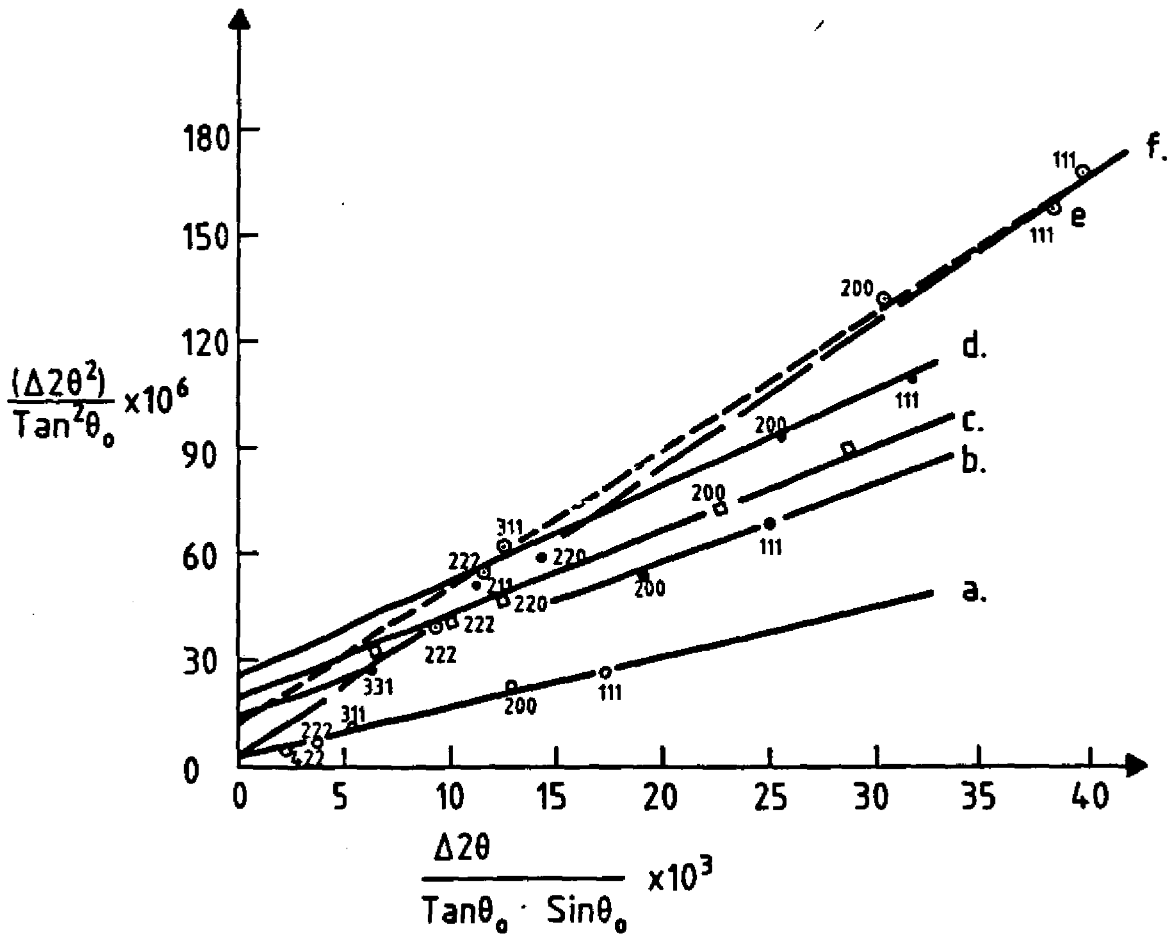

Fig. 8

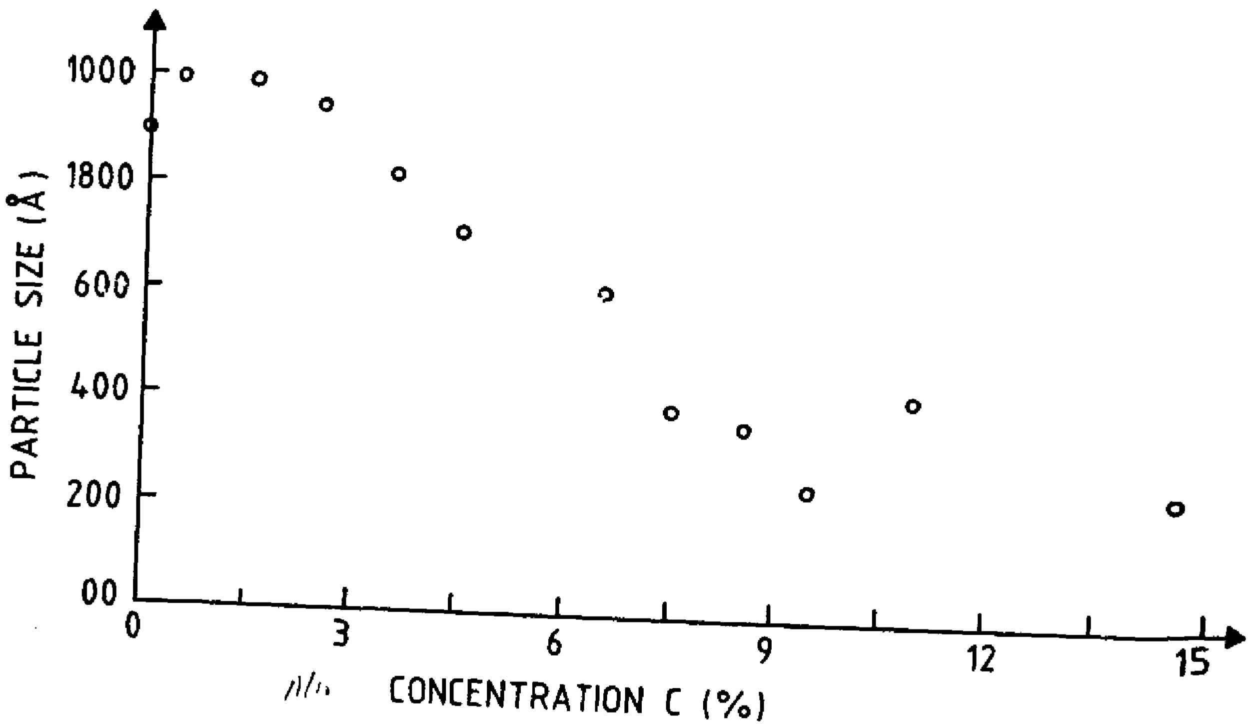

Fig. 9

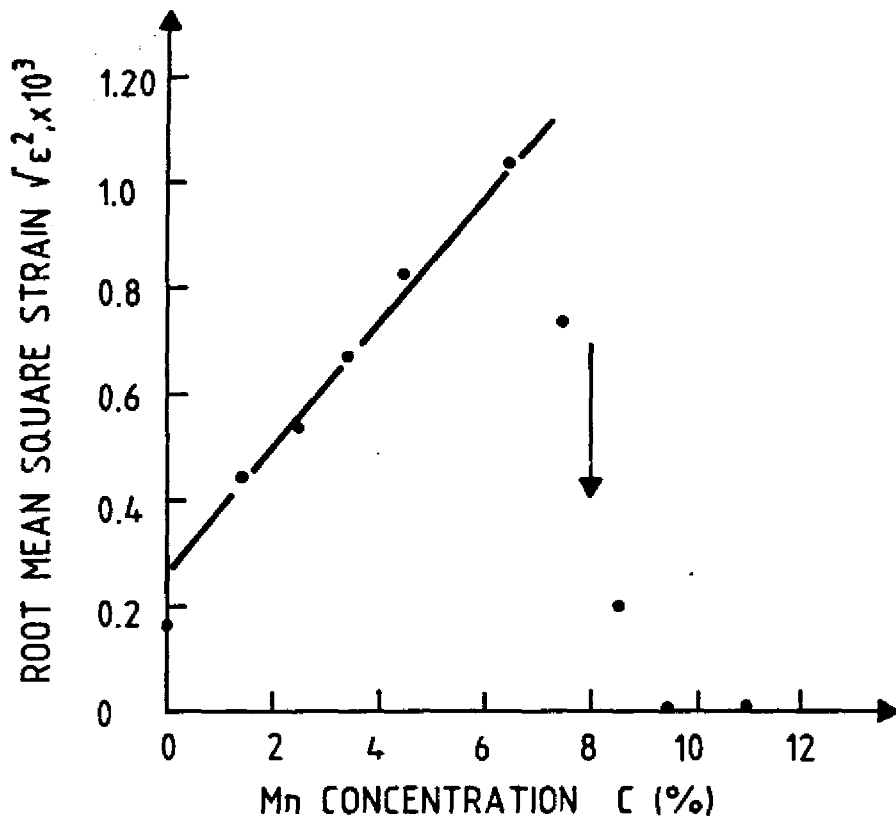

Fig. 10